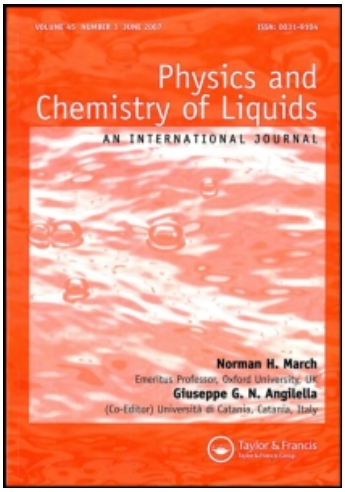

Physics and Chemistry of Liquids
Publication details, including instructions for authors and subscription information:
http://www.informaworld.com/smpp/title~content=t713646857

Density Fluctuations in Liquid and Polycrystalline Aluminium: A New Analysis of Old Neutron Scattering Data

Karl-Erik Larsson[a]
[a] Royal Institute of Technology, Stockholm, Sweden

To cite this Article Larsson, Karl-Erik(1980) 'Density Fluctuations in Liquid and Polycrystalline Aluminium: A New Analysis of Old Neutron Scattering Data', Physics and Chemistry of Liquids, 9: 2, 117 — 141
To link to this Article: DOI: 10.1080/00319108008084771
URL: http://dx.doi.org/10.1080/00319108008084771

Phys. Chem. Liq., 1980, Vol. 9, pp. 117–142
0031-9104/80/0902-0117$04.50/0

Printed in the U.S.A.

Density Fluctuations in Liquid and Polycrystalline Aluminium

A New Analysis of Old Neutron Scattering Data

KARL-ERIK LARSSON

Royal Institute of Technology, 10044 Stockholm, Sweden

(*Received March 26, 1979*)

About twenty years ago slow neutron scattering studies were made on liquid and solid polycrystalline aluminium and it was observed that the scattered spectra from the two phases were very similar. This observation formed the start of a new development in the field of liquid atomic dynamics continuing even since then. The original observation was, however, never analyzed in detail.

In the light of modern theoretical developments a new analysis is made of the old data. Similarly the observations done in experiments with advanced spectrometers is integrated into a total new view of the old experiment. It is found that a rather detailed understanding of the data is arrived at. It is thus found that the liquid scattering picture is to a large degree dictated by the structural disorder combined with dynamic effects of self motion as well as of collective back flow effects. Comparison is made between results obtained from modern kinetic theories for fluids and older phenomenological models. A considerable harmony in the total view on the liquid dynamics is finally obtained.

The analysis shows that the old cold neutron studies have a great value in revealing details of the dynamics in liquids. A combination of such measurements at larger wave vector transfers and other studies at small wave vector transfers with advanced theories is necessary to arrive at a full understanding of the physics of the problem.

I INTRODUCTION

One of the puzzling observations in early neutron spectroscopy on the dynamics of atoms on both sides of the melting point of a substance was the spectra of polycrystalline and liquid aluminium first observed 1959 in Stockholm.[1] It was found that the neutron spectra from the two phases at 630°C in the solid, polycrystalline phase and at 677°C in the liquid phase practically coincided point by point over a wide range in energy- and momentum-transfer space.[2,3] This observation triggered much speculation regarding the nature of excitations in simple liquids like a liquid metal.

Could phonon-like modes of motion (of course strongly damped and anharmonic) exist in the liquid? What role could the structure of the liquid play in the observed scattering pattern?

Other similar studies by use of cold neutron scattering (incoming neutron energy smaller than 5 meV) on lead,[4] tin,[5] sodium[6] and other metals confirmed the shape of the scattering pattern and the similarity between polycrystalline and liquid scattering patterns for such small scattering angles, θ, that the κ-value for elastic scattering was smaller than the κ-value, κ_0, at the peak of the liquid structure factor, $S(\kappa)$.

Already before the event of the first scattering experiments on coherently scattering liquids Vineyard[7] had proposed the first theoretical model (the convolution approximation) for the scattering function $S(\kappa, \omega)$. Other phenomenological models were proposed[8] to improve upon Vineyards primary model, which was obviously too crude and could not describe data. Rather early attempts were made at generalization of the hydrodynamic equations to carry their validity down to the atomic scale.[9,10,11] By the aid of the memory function approach various attempts were made to write down a generalized Langevin equation for application to scattering data.[12,13,14] Methods used in other branches of physics, such as plasma physics, were mobilized to describe the scattering function: the mean field theory.[15,16,17] Finally kinetic methods aiming at a first principle description of the binary and higher order collective collisions were developed for $S(\kappa, \omega)$.[18,19,20] Many of these developments were stimulated by the new techniques of computer science, the molecular dynamics method of simulation of systems of nature.[21,22,23]

In parallel with these theoretical developments the introduction of new intense neutron sources and efficient spectrometers made new measurements meaningful.[24,25,26] It was now possible to use higher energy ingoing neutrons of good energy resolution to send into samples. When the scattering function $S(\kappa, \omega)$ was plotted for constant κ it was found that in general no side peaks corresponding to damped phonons were observed. Indeed such features were observed on liquid rubidium[25] and on fluid neon[26] but not on liquid argon.[24] Recently such Brilloin peaks were also seen beyond all doubt in liquid lead.[27] At most such "peaks" were observed to exist for smaller κ-values and they always vanish for a κ-value around half the distance to the main peak of the static structure factor if not earlier. The existence of these "peaks" of course are of greatest interest as they build up a dispersion relation, which bridges the gap between the long wavelength hydrodynamic domain and the zero sound region.

Still, however, the old studies with cold neutrons, which triggered a considerable mental effort, have not obtained a detailed explanation. It has even been argued that such measurements involving larger energy and momentum

transfers are useless for various reasons. Partly because they were presented on a time-of-flight scale and partly because they were never properly corrected for multiple scattering.[28] The latter correction can nowadays be made with some confidence by computer technique, but was almost impossible to treat even approximately correct before 1965. It has been argued that only such studies, which result in a three peak structure, when presented on a constant κ-plot are of interest to reveal the possible existence of collective atomic motions. It was therefore felt that a modern approach to the interpretation of the old cold neutron data on liquid aluminium could be of interest. If an understanding could be reached, this would be applicable also to other similar observations.

II THE OBSERVATION

The neutron scattering experiment presently discussed was performed in a revised version 1962–63 (the first was made 1958–59) using a cold neutron spectrum impinging upon a sample of slab type with a thickness of 12 mm in the polycrystalline case and 17 mm in the liquid case. The mean free path of thermal neutrons in aluminium is of order 11 cm. The slab had an area of 100 cm^2 and was oriented at 45° with respect to the incoming beam. This orientation of the sample ensured that approximately the same area was seen at 20° as well as 60° angle of observation. The thickness of the molybdenum plates holding the sample in position was 0.1 mm in the polycrystalline case and 1 mm in the liquid case. Heating wires were wound round the ceramic frame holding the molybdenum plates and the whole container was kept in a vacuum vessel. The scattered beam was analyzed by a chopper and detectorbank situated after the sample in a neutron shielded arm. A more detailed account of the experimental conditions is given elsewhere.[3,29]

An example of the primary time-of-flight data at 60° angle of observation on polycrystalline and liquid aluminium are reproduced in Figure 1. It is particularly to be noted that the background runs, build up of various components as discussed in detail in Ref. 3, were normalized to the very short flight time region round 55 μsec/m, which corresponds to the fast neutron background transmitted by the chopper. This in general gave a slightly overestimated value of this background because part of it was due to multiple scattering not identified in these early measurements. This means that the resulting experimental data corrected for all backgrounds and exemplified in Figure 2 for 60° angle of observation are partly overcorrected. Thus there should be a slightly more pronounced tail for flight-times (or energy transfers) longer than ~ 850 μsec/m (or about $\Delta\omega < 1.5 \cdot 10^{13}$ rad/s). A similar effect should be even more pronounced at 20° angle of observation, which

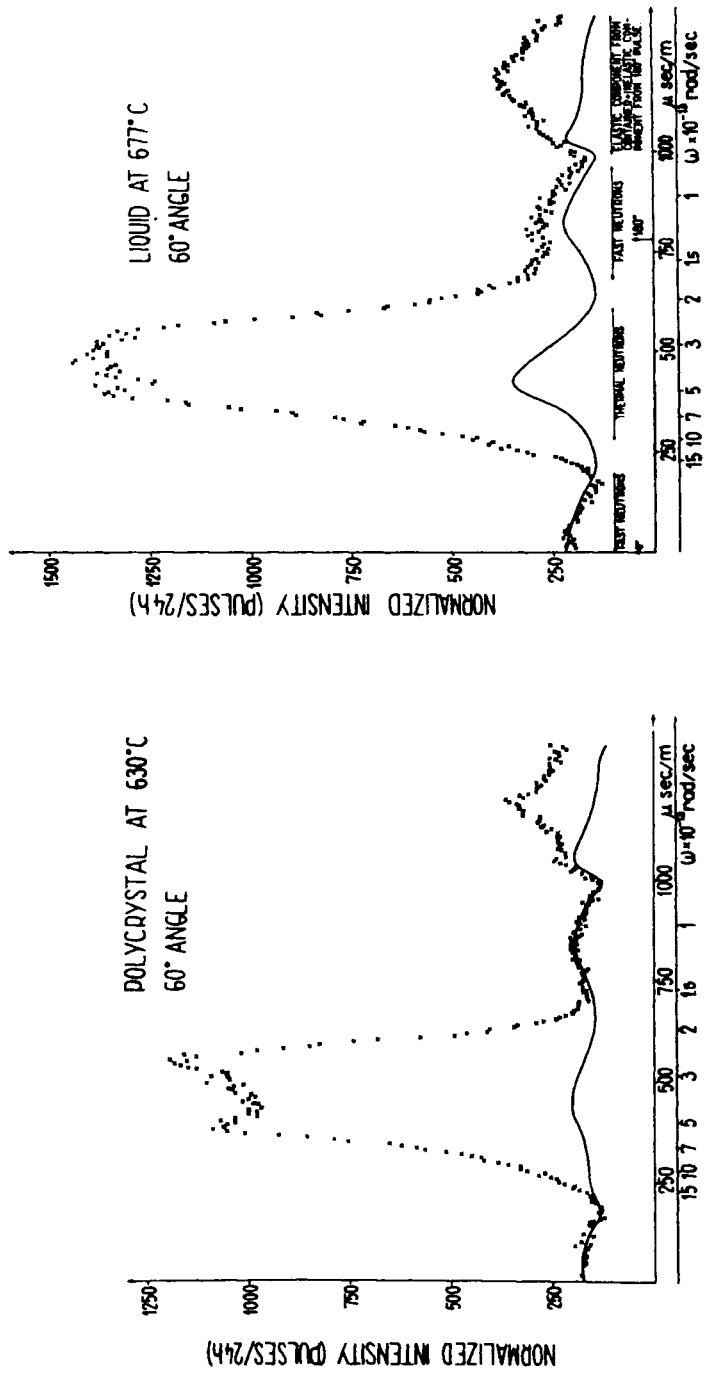

FIGURE 1 Primary scattering data from solid and liquid aluminium at 60° angle of observation. Backgrounds and its origin is indicated in the figure.

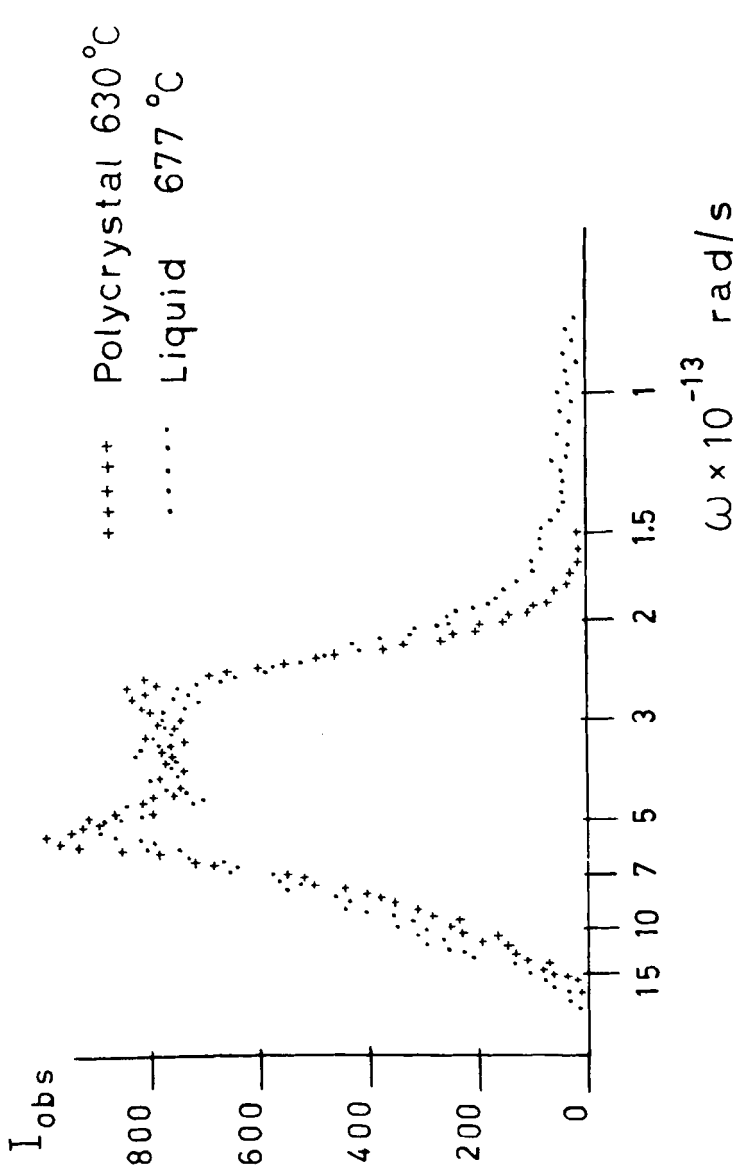

FIGURE 2 Corrected spectra from polycrystal and liquid aluminium close to the melting point. 60° angle of observation.

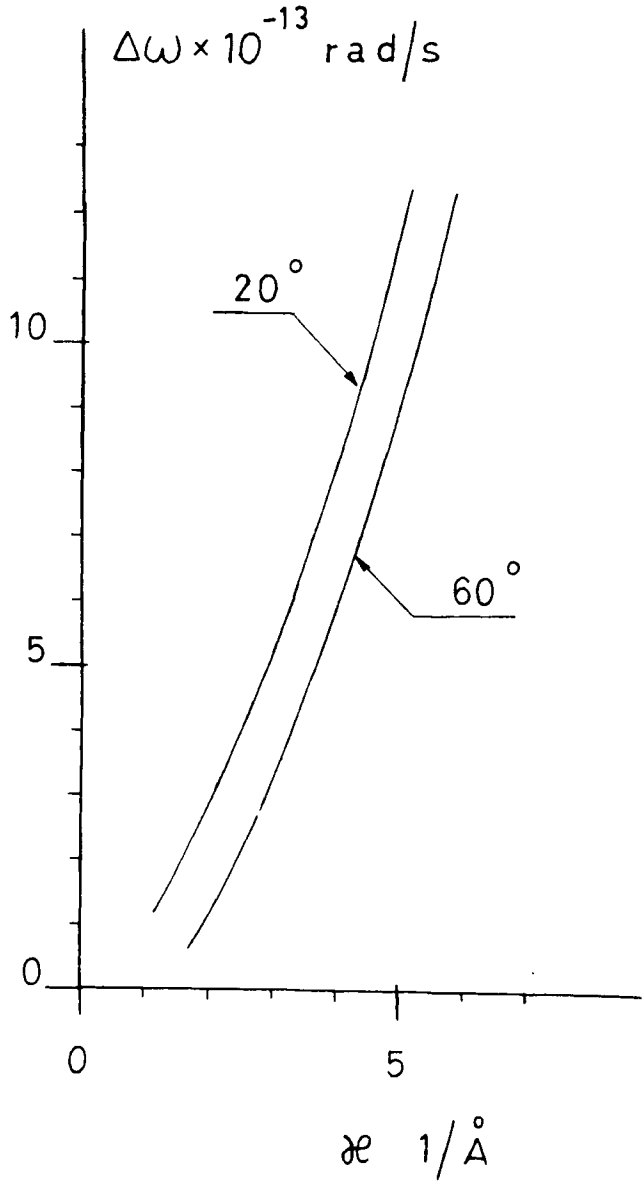

FIGURE 3 Loci in $(\kappa, \Delta\omega)$-plane for observations at 20° and 60° angle of observation.

involves even smaller intensities of first order scattering thus giving way for a higher second order scattering, relatively speaking.

The obvious first step to take is to perform a reasonably reliable multiple scattering correction. As the present observations trace out a path in the $(\kappa, \Delta\omega)$-plane as shown in Figure 3, it is clear that the scattering function will take on small values compared to its maximum values along the ridge, for which $\Delta\omega = 0$. Therefore the percentage multiple scattering should be high. Under such circumstances it is extremely important to use as an input kernel in the multiple scattering calculation a scattering function, which comes very near the true value. Also we shall not try to correct the experimental data. Instead we shall correct the theoretical scattering function for multiple scattering and compare the compounded calculated result, including first and second scattering, with observation. The most realistic scattering function one can select for liquid aluminium at present is the one calculated by Sjögren[30] and based on a molecular dynamics study of Ebbsjö and Waller.[31] The theory by Sjögren–Sjölander will be discussed in detail later.

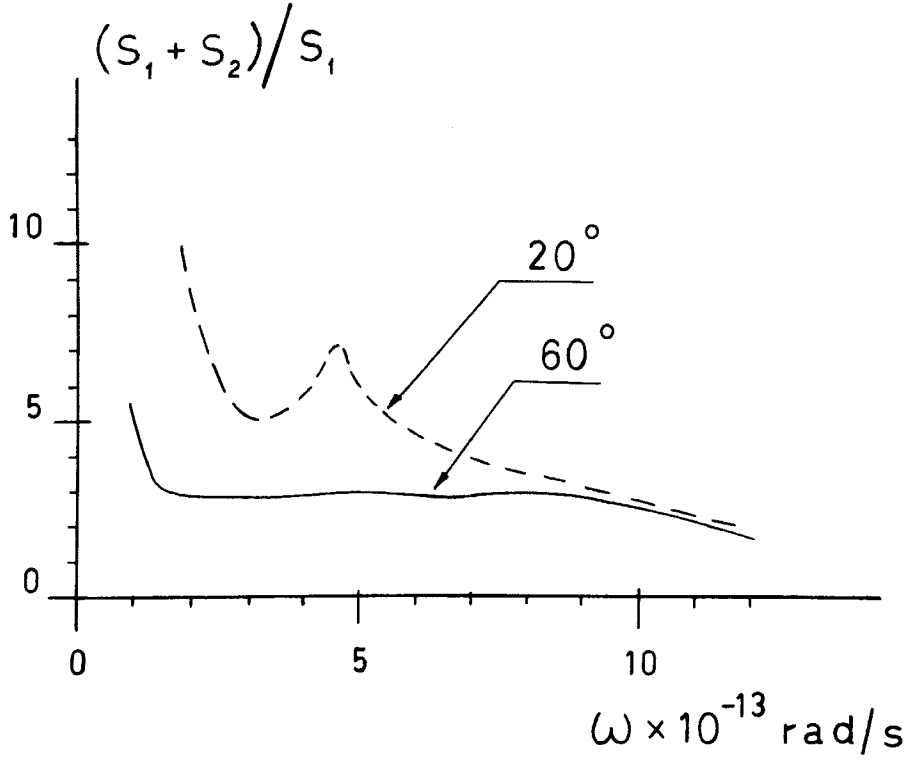

FIGURE 4 Calculated ratios of single + multiple scattered intensity, $S_1 + S_2$, to the single scattering, (S_1), at 60° and 20° angle of scattering.

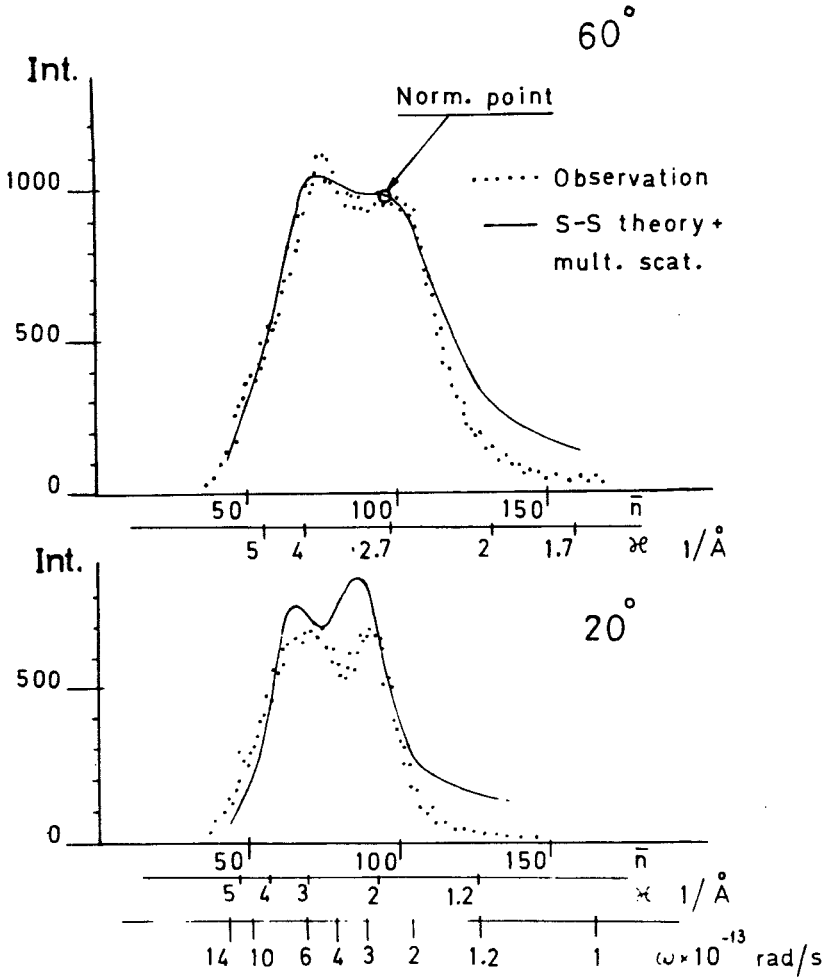

FIGURE 5 The theoretically calculated intensity distributions from liquid aluminium including multiple scattering corrections compared to observed intensity distributions at 60° and 20° angle of observation. Normalization at $\kappa = 2.7$ Å^{-1} at 60° angle.

To make the calculation reasonably simple the program developed by Cooking was used.[40] The ratio between singly (S_1) plus doubly (S_2) scattered neutrons to singly (S_1) scattered is given in Figure 4. As expected the multiple scattering is considerable, S_2/S_1 being about = 2 at 60° angle of observation and of order 4–5 at 20° angle within the energy transfer regions of interest as defined by the curves in Figure 3.

The crucial test is now to compare the calculated value $S_1 + S_2$ with the observed ones. This is done in Figure 5. The calculated values of $S_1 + S_2$ are

arbitrarily normalized to channel number 100 at 60° angle of observations equivalent to an energy transfer $\Delta\omega$ of $2.4 \cdot 10^{13}$ rad/s, where for this angle there is a first maximum in the observed intensity distribution.

It is seen that there is a remarkable similarity between the theoretical and experimental curves at 60° angle, the main discrepancy between the curves appearing for small energy transfers, where the overcorrection of the experimental data for background discussed above is expected to give the largest effect. Also at 20° angle the agreement is reasonable remembering the larger effect of overcorrection for backgrounds at this angle. It is seen that the two-peak structure is reproduced and the general conclusion to be drawn is that if the primary measurement had been better corrected for background, the theoretical curves would have fitted the experiment within limits of accuracy, say $\pm 10\%$ allowing for uncertainties in corrections, multiple scattering calculation and statistical counting errors.

In order to get a feeling for the effect of the topological shape of the total $S(\kappa, \Delta\omega)$ scattering surface on the particular cut with the locus of the 60° angle of observation in the $(\kappa, \Delta\omega)$-plane, a threedimensional plot is given of both $S(\kappa, \Delta\omega)$ and $\omega^2 S(\kappa, \Delta\omega)$ along this line (Figure 6a and b). Here $\hbar\Delta\omega$ is the energy gain of outgoing, scattered neutrons of energy $h\omega$. In both figures the static structure factor is also given along the κ-axis. The theoretical values of $S(\kappa, \Delta\omega)$ are those calculated by Sjögren.[30]

It is observed from Figure 6a that for smaller momentum and energy-transfers $S(\kappa, \Delta\omega)$ drops sharply due to the dominans of the value of the static structure factor $S(\kappa)$ in this range, say $\kappa < 2$ Å^{-1}. (The peak of the structure factor occurs at $\kappa = 2.7$ Å^{-1}). In Figure 6b is shown how the second peak in the observation, which is proportional to exactly $\omega^2 S(\kappa, \Delta\omega)$, is a pure time-of-flight effect. For comparison the frequency distribution of the normal modes in solid aluminium at 80°K is shown along the $\Delta\omega$-axis. Remembering the primary observation exemplified in Figure 2 the observed spectrum from the polycrystal is almost coinciding with the theoretical one for the liquid shown in Figure 6b. It is of interest to note that the main intensity contribution to $\omega^2 S(\kappa, \Delta\omega)$ for $0 < \Delta\omega < 5 \cdot 10^{13}$ rad/s in the solid at low temperature corresponds to phonons of transversal nature. Only a minor region for $5 < \Delta\omega < 6$ is dominated by phonons of longitudinal nature.

III THEORETICAL IMPLICATIONS

There are three steps of theoretical refinement, which have occurred over a period of twenty years, in the description of atomic motions in fluids.

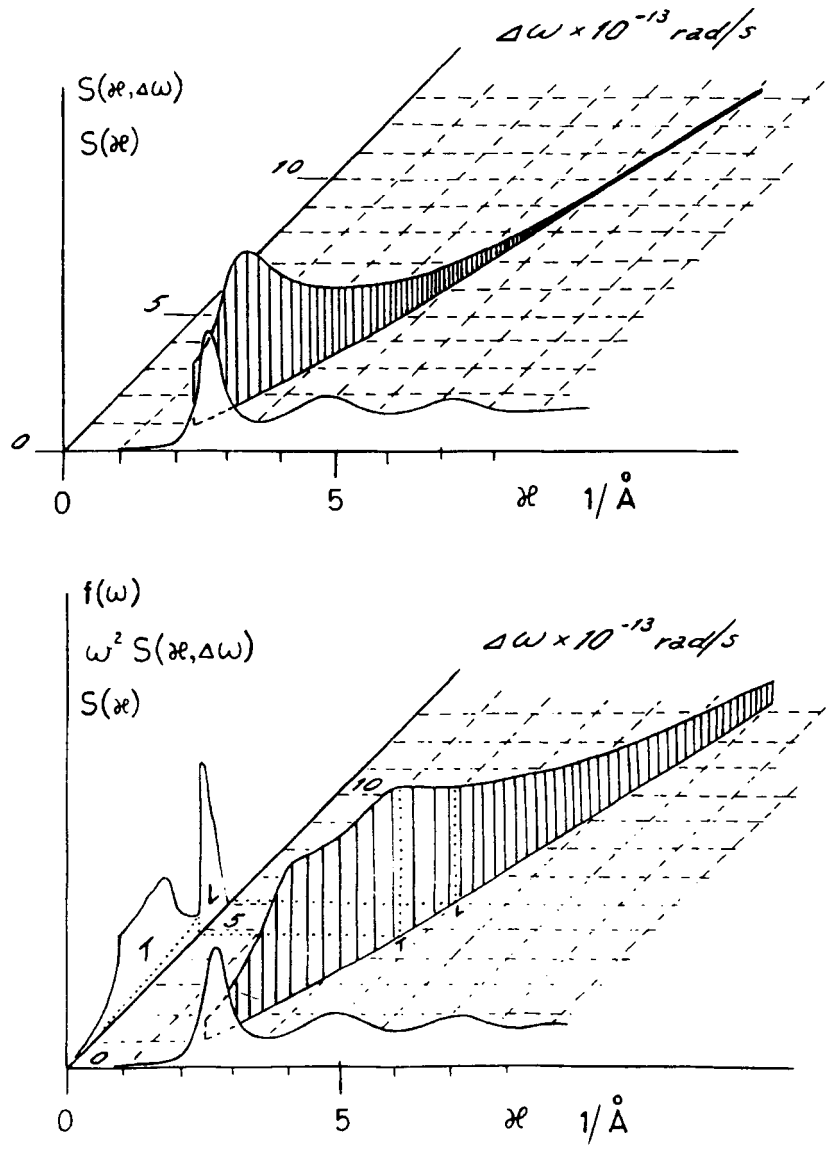

FIGURE 6 (a) The cut between the locus of the 60° angle in the $(\kappa, \Delta\omega)$-plane with the scattering surface $S(\kappa, \Delta\omega)$ calculated from the Sjögren–Sjölander theory. $S(\kappa)$ given in the $S(\kappa) - \kappa$-plane. (b) The same cut with the surface $\omega^2 S(\kappa, \Delta\omega)$ observed in a time-of-flight experiment. $S(\kappa, \Delta\omega)$ from same theory. $S(\kappa)$ given in $S(\kappa) - \kappa$-plane and $f(\omega)$ in $f(\omega) - \Delta\omega$-plane. T stands for transversal and L for longitudinal.

The first is the convolution approximation.[7] We shall use the notations used by Sjögren and Sjölander

$$S(\kappa, \Delta\omega) = \frac{1}{\pi} \operatorname{Re} F(\kappa, z = i\Delta\omega) \tag{1}$$

Then the convolution approximation reads

$$F(\kappa, z)_1 = S(\kappa)F_s(\kappa, z) \tag{2}$$

In this approximation the correlation hole round each atom follows the atom rigidly and the dynamics is entirely governed by the single particle motion determining $F_s(\kappa, z)$. All aspects of collective motion are lost.

The second approximation is the mean field approach. Various forms of this theory were discussed and its physical meaning analyzed.[32,33,17,20] An approximate but consistent form of it gives[33,20]

$$\begin{aligned} F(\kappa, z)_2 &= S(\kappa)F_s(\kappa, z) - S(\kappa)F_s(\kappa, z)\frac{nc(\kappa)(zF_s(\kappa, z) - 1)}{1 + nc(\kappa)(zF_s(\kappa, z) - 1)} \\ &= F(\kappa, z)_1 - C_1(\kappa, z) \end{aligned} \tag{3}$$

where $nc(\kappa) = 1 - 1/S(\kappa)$ is the direct correlation function. Here $F(\kappa, z)$ is purposely written as a sum of the convolution approximation term and a correction term, $C_1(\kappa, z)$. As shown by Sjögren and Sjölander the physical contents of this approximation is that a disturbance in the medium is propagated as if the marked central atom under observation would not cause any specific effect in its immediate surrounding. The atoms move in a mean field and there are no effects of backflow following upon hard core collisions. The memory of previous collision history is neglected.

In the third approximation, which we call the kinetic approach,[20] care is taken (to a certain approximation) also of the memory effects. The scattering function is obtained from

$$\begin{aligned} F(\kappa, z)_3 &= S(\kappa)F_s(\kappa, z) - S(\kappa)F_s(\kappa, z) \\ &\quad \times \frac{nc(\kappa)(zF_s(\kappa, z) - 1)}{1 + \left\{nc(\kappa) - \dfrac{\beta mz}{\kappa^2}\Gamma^d_{11}(\kappa, z)\right\}\{zF_s(\kappa, z) - 1\}} \\ &\quad - S(\kappa)\frac{\dfrac{\beta mz}{\kappa^2}\Gamma^d_{11}(\kappa, z)(zF_s(\kappa, z) - 1)(1 - F_s(\kappa, z))}{1 + \left\{nc(\kappa) - \dfrac{\beta mz}{\kappa^2}\Gamma^d_{11}(\kappa, 2)\right\}\{zF_s(\kappa, z) - 1\}} \\ &= F(\kappa, z)_1 - C'_1(\kappa, z) - C'_2(\kappa, z) \end{aligned} \tag{4}$$

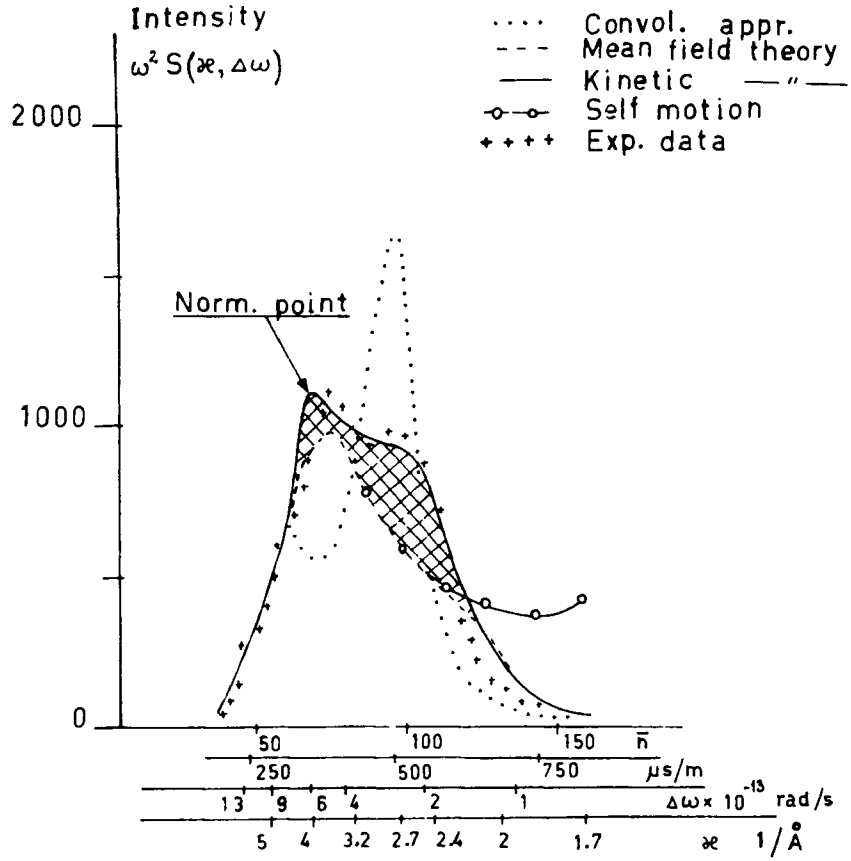

FIGURE 7 Calculated values of $\omega^2 S(\kappa, \Delta\omega)$ corresponding to 60° angle of observation based on three different degrees of theoretical approximation: covolution approximation, mean field approximation and kinetic theory. Also shown is $\omega^2 S_s(\kappa, \Delta\omega)$. The experimental observation uncorrected for multiple scattering is also shown (compare text on this point).

Here $\beta = 1/k_B T$, m = mass of the atoms and $\Gamma^d_{1,1}(\kappa, z)$ is a memory function containing two main contributions: one part is of first order in density and includes the effects of binary collisions, the other part is of second order in density and is caused by correlations between more than two particles. Backflow effects are approximately taken care of.

It is to be observed that it is just this third and highest approximation, which fits the aluminium data under discussion. A comparative study was made of the three models—mainly a comparison between the mean field model and the kinetic one as the convolution approximation is too crude as will be shown. With the same absolute normalization for the three models they are all exposed in Figure 7 and compared to the observation. They were

calculated along the locus in $(\kappa, \Delta\omega)$-space for the 60° angle of observation. Only single scattering (S_1) is included in the theoretical models. The experimental observation is given without multiple scattering correction. This correction does not change the *shape* of the observed intensity distribution because S_2/S_1 is approximately constant over the observed $\Delta\omega$- and κ-range for 60° angle (Figure 4). The following facts are observed:

1) The convolution approximation cannot describe data.

2) The mean field theory in its approximate form giving a wrong fourth frequency moment of $S(\kappa, \Delta\omega)$ gives a poor description of data.

3) For a κ-value < about 2.2 Å^{-1} the mean field and the kinetic theories practically coincide and are both determined to a large degree by the static structure factor, which decreases rapidly for $\kappa < 2.2\ \text{Å}^{-1}$. $S(\kappa, \Delta\omega)$ is guided by the factor $\{S(\kappa)\}^2 S_s(\kappa, \Delta\omega)$.

4) For a κ-value > about 2.2 Å the mean field theory practically coincides with $S_s(\kappa, \Delta\omega)$ for the energy transfers involved here and the dynamics is thus altogether described by the self-motion. No or very small collective effects are involved in the mean field theory in this domain.

5) The kinetic theory, which relatively well describes data, has an additional component (cross hatched area in Figure 7) corresponding to the back flow term dominated by the memory component $\Gamma^d_{11}(\kappa, \omega)$. It is exactly this component in the kinetic form of scattering function, which creates the good fit to the experiment.

The result of the calculations is that the kinetic theory describes the observed data well and the mean field theory in the consistent form Eq. (3) does not.

IV FURTHER ANALYSIS

Due to the conclusions of the previous section it is of interest to further analyze, which terms in Eqs. (3) and (4) are of importance in various κ and $\Delta\omega$-regions. Therefore the "correction terms" $C_1(\kappa, \omega)$ of Eq. (3) and the term $C_2'(\kappa, \omega)$ of Eq. (4) were extracted from the mean field scattering function Eq. (3) and from Sjögrens calculations of $S(\kappa, \Delta\omega)$ from Eq. (4) in the following way.

From Eq. (3) it is seen that in the mean field approach the scattering function may be written

$$S(\kappa, \Delta\omega)_{m.f.} = S_s(\kappa, \Delta\omega) f(\kappa, \Delta\omega) \tag{3'}$$

Similarly one may write for the kinetic scattering function

$$S(\kappa, \Delta\omega)_{\text{kin}} = S_s(\kappa, \Delta\omega)g(\kappa, \Delta\omega) \tag{4'}$$

From these definitions one derives the identity

$$\begin{aligned} S(\kappa, \Delta\omega)_{\text{kin}} &= S_s(\kappa, \Delta\omega)\{S(\kappa) + (f(\kappa, \Delta\omega) - S(\kappa)) \\ &\quad + (g(\kappa, \Delta\omega) - f(\kappa, \Delta\omega))\} \\ &= S_s(\kappa, \Delta\omega)\{S(\kappa) + C_1''(\kappa, \Delta\omega) + C_2''(\kappa, \Delta\omega)\} \end{aligned} \tag{5}$$

Here

$$C_1''(\kappa, \Delta\omega) = \frac{C_1(\kappa, \Delta\omega)}{S_s(\kappa, \Delta\omega)} \tag{5.1.}$$

$$C_2''(\kappa, \Delta\omega) \simeq \frac{C_2'(\kappa, \Delta\omega)}{S_s(\kappa, \Delta\omega)} \tag{5.2.}$$

The first correction term, $C_1''(\kappa, \Delta\omega)$ brings the convolution approximation into the mean field form and is exact. The second term evaluated in the way given by Eq. (5) does not give $C_2''(\kappa, \Delta\omega)$ exactly because $f(\kappa, \Delta\omega)$ contains $C_1(\kappa, \Delta\omega)$, whereas $g(\kappa, \Delta\omega)$ contains $C_1'(\kappa, \Delta\omega)$, which differ in the term containing the memory function $\Gamma_{11}^d(\kappa, \Delta\omega)$ in the denominator. Eq. (5.2.) involves the assumption that the effect of the term containing $\Gamma_{11}(\kappa, \Delta\omega)$ in the denominator of $C_1'(\kappa, \Delta\omega)$ of Eq. (4) is small in the $(\kappa, \Delta\omega)$-domain of interest here with κ-values of order of κ_0 or larger (κ_0 is the value of κ at the main peak of the static structure factor). If this term is neglected in $C_1'(\kappa, z)$ of Eq. (4) one finds that $C_1'(\kappa, z) = C_1(\kappa, z)$ of Eq. (3).

The function $f(\kappa, \Delta\omega)$ is calculated using the mean field expression and has the form

$$f(\kappa, \Delta\omega) = \frac{[S(\kappa)]^2}{[1 + (S(\kappa) - 1)\omega b]^2 + a^2\omega^2(S(\kappa) - 1)^2}, \tag{6}$$

where

$$a = \frac{1}{\pi}\int_0^\infty e^{-\kappa^2\rho(t)} \cos \omega t \, dt$$

$$b = \frac{1}{\pi}\int_0^\infty e^{-\kappa^2\rho(t)} \sin \omega t \, dt$$

and

$$\rho(t) = \int_0^t dt'(t - t')\langle v(0)v(t')\rangle$$

The velocity correlation function is taken from Sjögrens computations.[30] The static structure factor used is the one obtained by Ebbsjö *et al.*[31] The

knowledge of $f(\kappa, \Delta\omega)$ and $S(\kappa)$ gives $C_1''(\kappa, \Delta\omega)$. Next $g(\kappa, \Delta\omega)$ is obtained from Sjögrens calculation of $S(\kappa, \Delta\omega)$ and $S_s(\kappa, \Delta\omega)$ according to Eq. (4'). From the knowledge of $g(\kappa, \Delta\omega)$ and $f(\kappa, \Delta\omega)$ the factor $C_2''(\kappa, \Delta\omega)$ is obtained according to Eq. (5). In Figure 8 the approximate forms of $C_1''(\kappa, \Delta\omega)$ and $C_2''(\kappa, \Delta\omega)$ are given for $1 \cdot 10^{13} < \omega < 8 \cdot 10^{13}$ rad/s. In the same figure the factor $1 - S(\kappa)$ is also shown for comparison. It is observed that for $\Delta\omega \geq 2 \cdot 10^{13}$ rad/s the factor $C_1''(\kappa, \Delta\omega)$ coincides with $1 - S(\kappa)$. This means that the kinetic scattering function can in that region be written

$$S(\kappa, \Delta\omega)_{\text{kin}} \simeq S_s(\kappa, \Delta\omega)\{1 + C_2''(\kappa, \Delta\omega)\} \tag{7}$$

So at least for $\kappa > 2\,\text{Å}^{-1}$ (when $S(\kappa)$ is of order one) and $\Delta\omega > 2 \cdot 10^{13}$ rad/s the scattering function essentially consists of a sum of two terms, the self part $S_s(\kappa, \Delta\omega)$ and the collision part, $C_2''(\kappa, \Delta\omega)S_s(\kappa, \Delta\omega) = C_2'(\kappa, \Delta\omega)$. As shown by the analysis performed by Sjögren,[20] Sjölander[20] and especially by Sjödin[33] for the large $\Delta\omega$-values ($\Delta\omega > 1 \cdot 10^{13}$ rad/s) involved in these observations, it is only the first rapidly decaying part of the memory function $\Gamma(t)$, which plays any role. With other words: the second term in Eq. (7) corresponding to the cross-hatched area of Figure 7 contains information on the details of the binary collision process and therefore at least also on the repulsive part of the pair potential. Sjödin in a recent paper[33] states that the mean field theory is found to give a good description of $S(\kappa, \Delta\omega)$ beyond $\kappa = \kappa_0$. The present observation is not in agreement with this statement. As a matter of fact Figure 5 of Sjödins paper shows significant differences between the mean field result and the molecular dynamics result even for $\kappa > \kappa_0$. These discrepancies are magnified in the present way of presenting and analyzing the data.

In order to further shine some light on the difference between the mean field results and the kinetic results the factors

$$f(\kappa, \Delta\omega) = \frac{S(\kappa, \Delta\omega)_{\text{m.f.}}}{S_s(\kappa, \Delta\omega)} \quad \text{and} \quad g(\kappa, \Delta\omega) = \frac{S(\kappa, \Delta\omega)_{\text{kin}}}{S_s(\kappa, \Delta\omega)}$$

are plotted in a three-dimensional plot as a function of $\Delta\omega$ for a few κ-values (Figure 9a and b). In this way of plotting the results, the ratio $S(\kappa, \Delta\omega)/S_s(\kappa, \Delta\omega)$ forms a surface above the $(\kappa, \Delta\omega)$-plane. When $S(\kappa, \Delta\omega) \sim S_s(\kappa, \Delta\omega)$ this surface degenerates into a plane parallel to the $(\kappa, \Delta\omega)$-plane. The difference between the two theories is obvious, the first being mainly structure dominated, the second in addition depending upon a frequency dependent memory effect mainly due to binary collisions. As the shaded areas are riding on a surface determined by the self part, $S_s(\kappa, \Delta\omega)$, it is obvious that an accurate knowledge of the self motion of atoms is necessary, if the total scattering functions, $S(\kappa, \Delta\omega)$, should be correctly described.

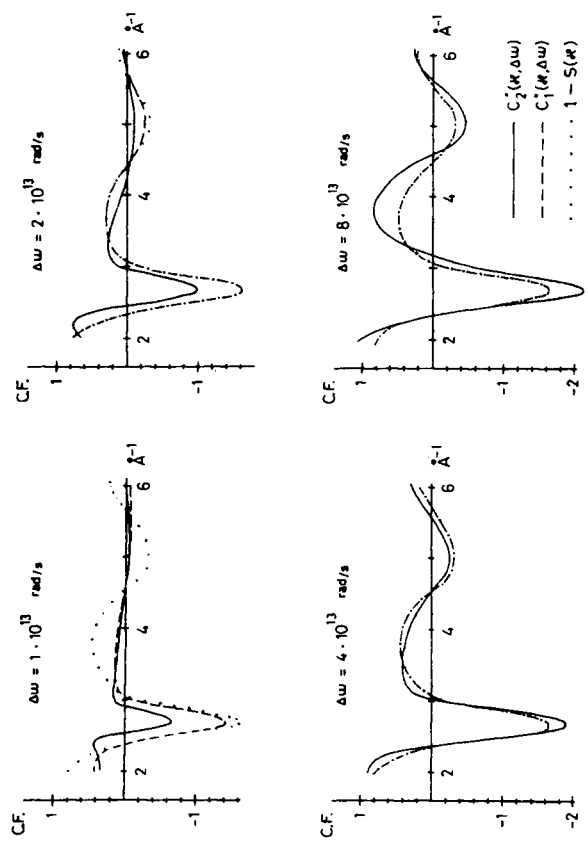

FIGURE 8 Examples of the "correction factors" (C.F.) $C_1''(\kappa, \Delta\omega)$ and $C_2''(\kappa, \Delta\omega)$ converting the convolution approximation into mean field and kinetic theory approximations. Also shown is $1 - S(\kappa)$.

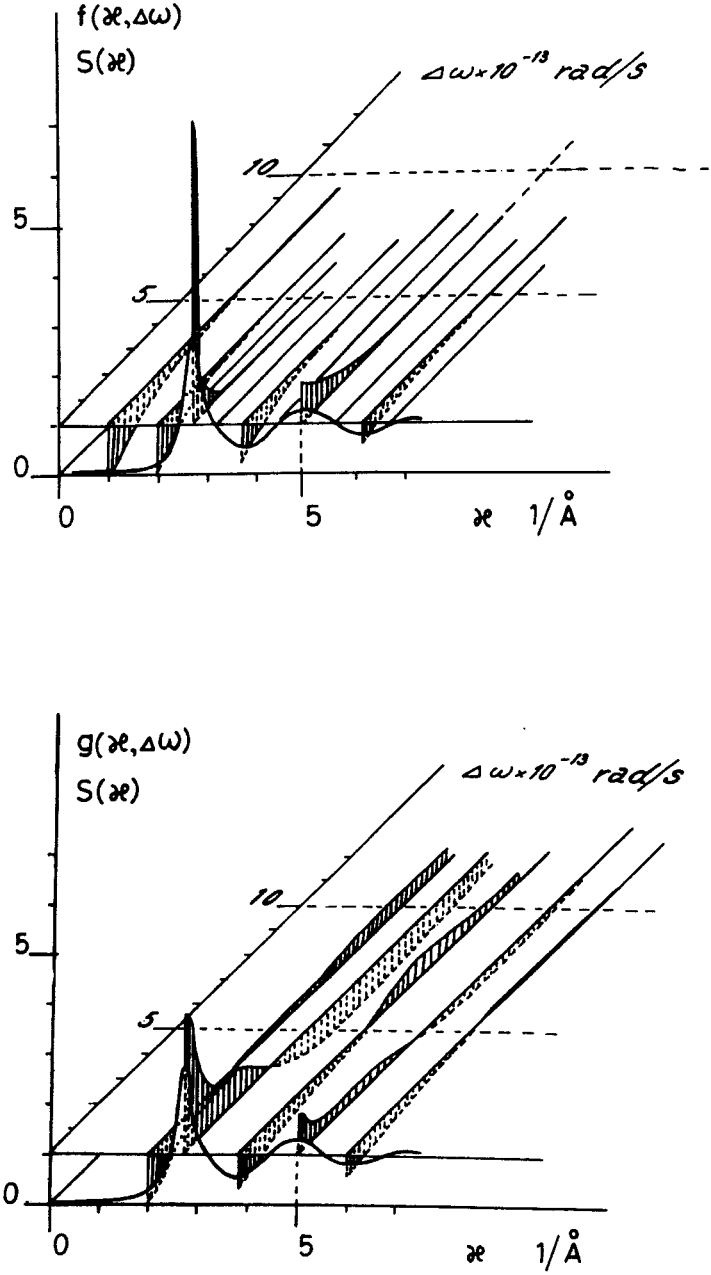

FIGURE 9 Plot of the ratio $S(\kappa, \Delta\omega)/S_s(\kappa, \Delta\omega)$ for $S(\kappa, \Delta\omega)$ calculated on the basis of two different theories (a) mean field theory (b) kinetic theory. The ratio is exposed as a function of $\Delta\omega$ for a few κ-values. Also shown is $S(\kappa)$ in the $S(\kappa) - \kappa$-plane.

V OLDER PHENOMENOLOGICAL THEORIES AND SOLID-LIKE BEHAVIOUR

As mentioned in the introduction the early observations on liquid metals and liquid argon stimulated theoretical efforts. In the beginning these were concentrated to phenomenological models. An inspection of the forms of Eqs. (3), (4) and (5) reveals a striking formal similarity between them and the form constructed by Singwi.[8,34] He proposed a scattering function of the form

$$S(\kappa, \Delta\omega) = S(\kappa)S_s(\kappa, \Delta\omega) + H(\kappa, \Delta\omega)$$

which in a final version[34] can be given as

$$S(\kappa, \Delta\omega) = S_s(\kappa, \Delta\omega)\left\{S(\kappa) + \frac{1}{6}\left(\frac{\Delta\omega}{c}\right)^2 L(R, q, \kappa)\right\}$$

The physical idea was that for a very short time τ_0, of order 10^{-12} seconds or less the near surrounding of range R of order 10 Å to each atom does not change much. It takes time for the asymptotic diffusive behaviour with $\rho(t) = Dt$ to set in (D is self diffusion constant, t time). The atoms within this little sphere of coherence were assumed to move as in a solid for the short time mentioned. This idea was based on observations like the present exemplified in Figure 1 and 2. The result was that a correction term, $H(\kappa, \Delta\omega) = S_s(\kappa, \Delta\omega) \cdot \frac{1}{6}(\Delta\omega/c)^2 L(R, q, \kappa)$ to the convolution approximation was derived, where c is the sound velocity and q is the quasi-phonon wave number. Outside the sphere of radius R the convolution approximation was assumed a reasonable approximation. The essential correction factor is $L(R, q, \kappa)$.

From the present calculations, as given by Eq. (5), it is possible to calculate $\{C_1''(\kappa, \Delta\omega) + C_2''(\kappa, \Delta\omega)\} \cdot c^2/(\Delta\omega)^2 = F(\kappa, \Delta\omega)$, which should be directly comparable to Singwis $L(R, q, \kappa)$. With $c = 4670$ m/s the factor $F(\kappa, \Delta\omega)$ was calculated for some $\Delta\omega$-values. The result is shown in Figure 10a. Qualitatively and even quantitatively the shape of the curves are indeed very similar to those of Singwis[35] (Figure 10b). In order to arrive at the curves of Figure 10b distinct values of q had to be guessed as well as a value of R. Several choices were tested and it was found that $R = 6$ Å is definitely too small, whereas $R = 25$ Å is too large to give reasonable values of the wave vector values q. A "reasonable" value is considered one, which gives a relatively good fit with the corresponding curve of Figure 10a. The important part of the curves is the region round $\kappa = \kappa_0 = 2.7$ Å, where structural effects are dominating. The deviation between the $L(R, q, \kappa)$-curve for the smallest q-value ($=0.27$ Å^{-1}) and the $F(\kappa, \Delta\omega)$-curve for the smallest $\Delta\omega$-value ($=1 \cdot 10^{13}$ rad/s) for κ-values larger than 3 Å^{-1} may be due to a too large computational step in the q-integration involved in $L(R, q, \kappa)$. (Compare

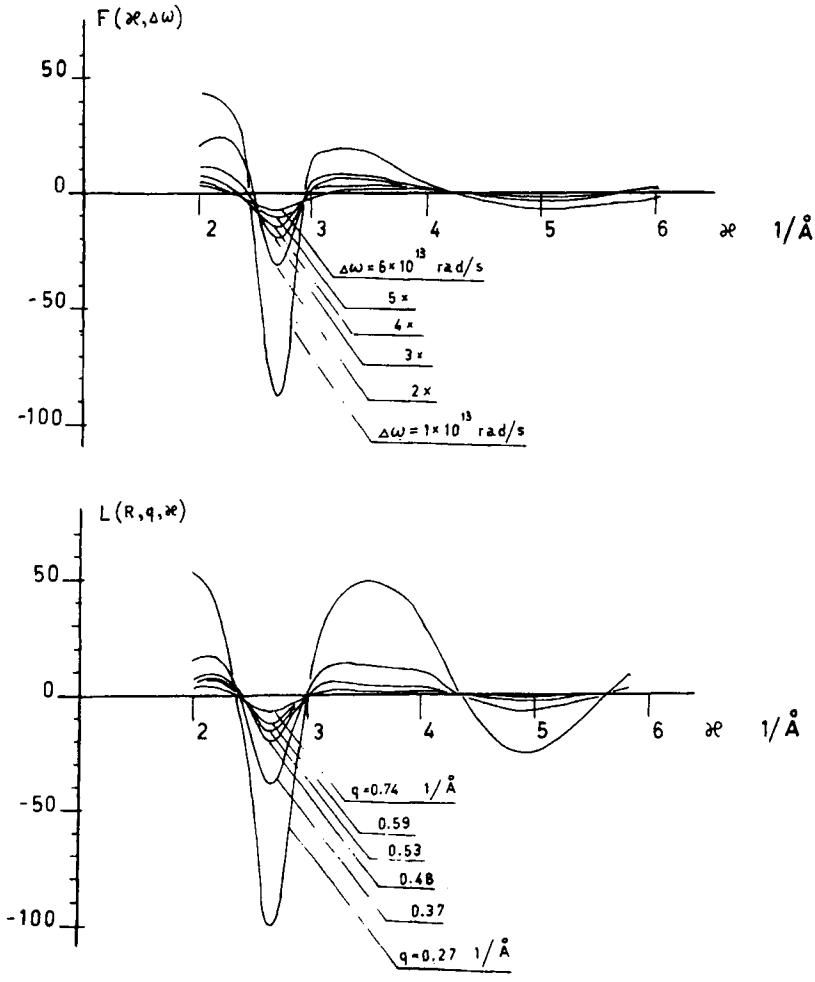

FIGURE 10 Two correction factors to convolution approximation (a) the kinetic theory correction factor = $F(\kappa, \Delta\omega) = 6c^2/(\Delta\omega)^2\{C_1''(\kappa, \Delta\omega) + C_2''(\kappa, \Delta\omega)\}$ (b) Singwis phenomenological approach. Correction factor = $L(R, q, \kappa)$. $R = 17$ Å.

Ref. 35, Eq. (45).) Disregarding this discrepancy the agreement is remarkable. It is of interest to combine the obtained q-values with corresponding $\Delta\omega$-values to construct a "dispersion relation." It is seen in Figure 11, where these pairs are combined, that an inconsistancy arises in the results. In Singwis derivation a Debye dispersion relation $\Delta\omega = c \cdot q$ was assumed. Only for the smallest q-values—($q < 0.3$ Å^{-1}) corresponding to wave length $\lambda > 20$ Å—is there an approximate agreement with the assumed sound velocity. At larger $\Delta\omega$-values the derived q-value—($q > 0.6$ Å^{-1}) corresponding to

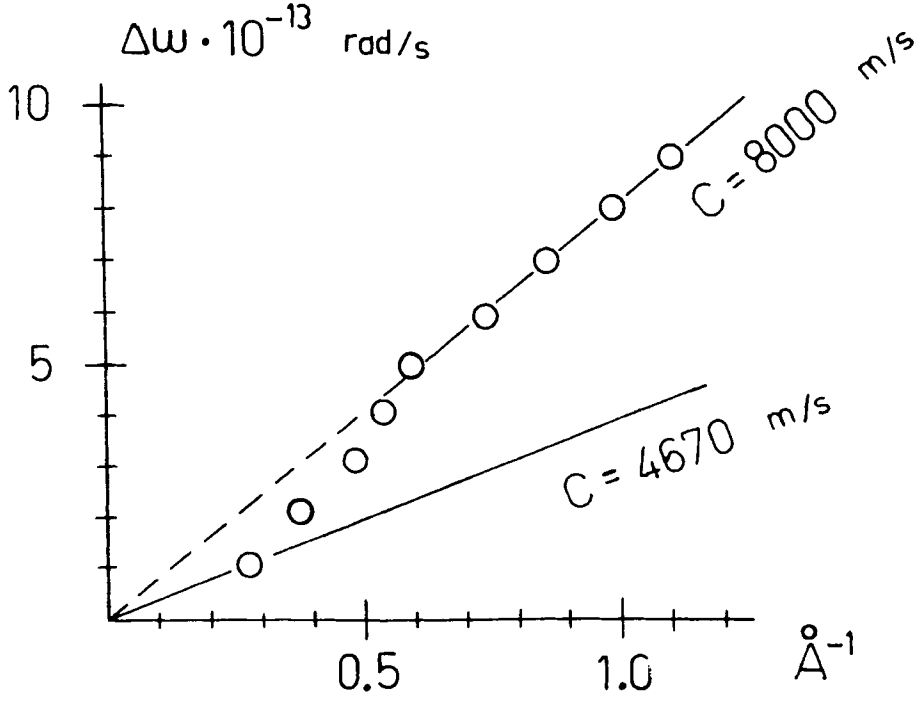

FIGURE 11 "Dispersion relation" for overdamped oscillations in a κ-range round $\kappa = \kappa_0$. Obtained from comparison of the curves of figure 10(a) and 10(b). Observe that these "dispersion curves" should start out from $\kappa = \kappa_0$.

$\lambda < 10$ Å—together with the corresponding $\Delta\omega$-values form pairs, which fall along a line with a slope corresponding to a velocity of 8000 m/s.

In this connection it is to be remembered that for $\Delta\omega \geq 2 \cdot 10^{13}$ rad/s it is the hard core collision that dominates in the memory function[34] and therefore also in the correction terms. The phonon analogy of Singwi requires more of the collective motions—real phonons. This is probably the reason why the noted inconsistency arises. There is little reason to expect the strongly damped high frequency disturbances of transient nature driven by a hard core collision to propagate with sound velocity. Considering the similarity between the curves of Figure 10a and 10b, it is not unreasonable to talk about an overdamped oscillatory motion or collective mode with $\lambda \sim R \sim 17$ Å and life time $\tau_0 \sim 2\pi/\Delta\omega \sim 3 \cdot 10^{-13}$ s. This is what is left of "solid-like-behaviour."

It should be observed that this observation is valid when $\kappa > \kappa_0$. When $\kappa \ll \kappa_0$ we end up in the upper regions of the hydrodynamic domain. Here $\kappa = q$ and the wave length may be $> R$. If one compares this statement with

Sjögrens calculations on aluminium one finds that the well defined side peaks (Brilloin dubletts) disappear round $q \sim 0.4\,\text{Å}^{-1}$ corresponding to $\lambda \sim 15\,\text{Å}$ and $\omega \sim 2 \cdot 10^{13}$ rad/s corresponding to a period of $2\pi/\omega \sim 3 \cdot 10^{-13}$ s. For shorter wave lengths and periods of oscillation the motion is overdamped.

How should this be understood? If the collective mode exists all the way from $q = 0$ to $q \sim 0.4\,\text{Å}^{-1}$. why is it overdamped in the range of $0.4\,\text{Å}^{-1} < q < \kappa_0/2 = 1.35\,\text{Å}^{-1}$? For the highest frequencies the liquid should appear with solid-like stiffness. The physical explanation of this fact must be that for wavelengths ($2\pi/q = \lambda$) $15\,\text{Å} < \lambda < 4.7\,\text{Å}$ the exact geometrical ordering of atoms plays a dominant role. In the solid phase there exists a periodic lattice, which is the carrier of the periodic disturbances of all wave lengths and particularly the shortest ones. If an atom is missing at a lattice position or very much displaced from its periodic structure site, the wave motion will be damped out. This is just what happens in a liquid. The lack of geometrical order in liquid aluminium is responsible for the overdamping of the highest frequency vibrations. From long wavelengths down to wavelengths of 15 to 20 Å the lack of order must be of smaller importance; one may still talk of motions of "volume elements" in the semi-macroscopic hydrodynamical sense. But shorter wavelength motions can only be described in a truely atomistic way. If this is done the waves cannot propagate in the highly disordered system.

These observations are in fair agreement with the study of mean life time and mean free path of phonons in high temperature aluminium performed about twenty years ago.[35] The mean life time, τ, of a phonon of a wavelength of 6–14 Å was found to be $\sim 4 \cdot 10^{-13}$ s. The corresponding vibrational period ($2\pi/\omega = 1/\nu$) was $\sim 2 \cdot 10^{-13}$ s. So in the solid the product $\nu\tau \sim 0.5 \cdot 10^{13} \cdot 4 \cdot 10^{-13} = 2$. Therefore the vibration is just barely defined even in the solid. In the liquid the vibration is overdamped due to geometrical disorder and $\nu\tau \leq 1$ because τ is short.

These conclusions seems to stand in sharp contrast to the spirit of Singwis model and the assumption of existing propagating high frequency modes within a range R round each atom in the liquid. As, however, is seen from the expression of $L(R, q, \kappa)$ it contains as an important element an integral guided by the structural term $S(\kappa) - 1$ describing pair correlations; this is modified by the damping function given in r-space as $\exp\{-r^2/R^2\}$ and by the allowed range of q-values. This term contains few elements of the dynamics of the motion. Similarly it is seen from Figure 8 and the associated discussion that the correction $F(\kappa, \Delta\omega)$ is approximately equivalent with $C_2''(\kappa, \Delta\omega)$, which varies with κ in a way that is mainly similar to $1 - S(\kappa)$ modified by effects due to the memory function Γ_{11}^d (compare Eqs. (3), (4) and (5) with Figure 8). The two factors $L(R, q, \kappa)$ and $F(\kappa, \Delta\omega)$ are rather

similar because in both structural effects dominate and the kinetic parts appear as small corrections added to the structure effects.

In Singwis phenomenological model as well as in the advanced kinetic model the total coherent scattering function is strongly determined by the form assumed for the self-motion. Already in the older phenomenological model $S_s(\kappa, \omega)$ was dominated by the Fourier transform of the velocity auto correlation function (vac), which is of course the case also in the sophisticated kinetic theory (see for intance Ref. 30, Eqs. 2.3–2.5).

A rather elucidating study of the nature of the vac in liquid metals and in a Lennard–Jones fluid was performed by Tsang and Maclin[38] and Tsang and Tang.[39] It was shown that the vac for short times ($\tau < 3 \cdot 10^{-13}$ s) may be derived from starting conditions that reminds of those in a solid. Furthermore the effective many-body-collision was approximated by a sum of a binary collision and an effect of the rest of the nearest neighbours. These later contributions to the forces were lumped together into a memory function term (in effect this is also the physical content of the more general treatment of Sjögren–Sjölander). It turned out that the vac calculated from this simple approach agreed very well with the vac obtained from molecular dynamics computations on liquid sodium and liquid argon. This simple argument again emphasizes the fact that for very short times the dynamic atomic behaviour of a liquid is not vastly different from that of a solid. It furthermore stresses that the important collision phenomenon is the binary collision. The effect of higher order collisions and collectivity related to these, as is evident from other work, is more related to the intermediate and long time behaviour of atomic dynamics.[23,20]

Finally we shall make a few further comments on the celebrated "solid behaviour" of liquid atomic motions. This idea got a strong support from observations like the present one but was later called into question, when more detailed observations were made allowing constant κ-plots even down to medium small κ-values. Such plots did in most cases not show any three-peak structure for κ-values $> \kappa_0/2$. A direct experiment set up to observe phonons in liquid lead corresponding to a q-value at the zone boundary of the corresponding solid gave a negative result.[36] On the other hand observations were made on phonon groups[35,37] in single crystals in the neighbourhood of the melting point showing that phonons could still be seen. They appeared, however, strongly damped with a mean life time of the order of $4 \cdot 10^{-13}$ s corresponding to not much more than one period. Or equivalently: the mean free path observed was of order one wavelength. This indicates that a considerable geometrical disorder exists in the solid near the melting point, say within 5–10% from the actual transition point.

This observation plus the observed phonon frequency shifts indicates that it is not relevant to correlate the frequency distribution $f(\omega)$ of normal modes

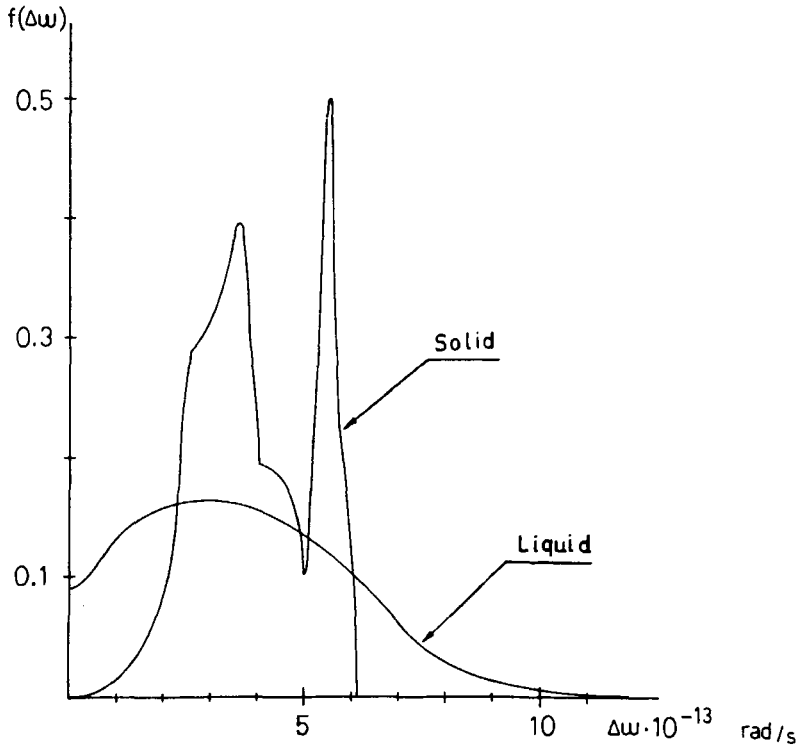

FIGURE 12 Frequency distribution $f(\Delta\omega)$ of normal modes in low temperature solid aluminium and the Fourier transform of the velocity auto correlation function in liquid aluminium.

at 80°K as in Figure 6b with $S(\kappa, \Delta\omega)$ for the liquid. In the liquid phase it is the spectral distribution of the velocity auto-correlation function, which is the relevant function. In Figure 12 this Fourier transform of $\langle v(0)v(t)\rangle$ for liquid aluminium[30] is given in comparison to the low temperature $f(\omega)$ for phonons. The difference is so dramatic that it is hardly meaningful to ask the question what happened to the phonons of transversal nature. Many modes went into diffusion for $\omega \to 0$, but there is also a tail of very high frequency modes in the liquid. Due to strong damping caused by geometrical disorder and large amplitude motions, the similarity between the atomic motions in the low temperature solid and in the liquid near the melting point is to a large degree lost. The centre-of-gravity of the two frequency distributions remain, however, about the same. This must be dictated by the shape of the interatomic potential. It is possible that $f(\omega)$ for the high temperature solid resembles the Fourier transform of $\langle v(0)v(t)\rangle$ for the liquid near the melting point. Furthermore the dominating multi-phonon terms in the spectrum from

the solid contribute to smear out the scattering pattern and may well contribute to create the resemblance between the solid polycrystalline and liquid scattering patterns.

The true nature of the excitations in the liquid phase is to some degree understood by the description of the kinetic theory showing the importance of the binary collision and the following backflow effects. The high temperature and high frequency phonons in the solid near melting with their very short mean free paths may in fact be quite similar in nature.

A very important and dominating effect on the two spectra from polycrystal and liquid, respectively, is caused by the static structure. In the case of the polycrystal no modes are observed for $\kappa < \tau - q$, where τ is the value of the smallest reciprocal lattice vector and q is the value of a phonon wave vector. This creates the intensity cut-off for smaller energy transfers. The same cut-off effect in the liquid case is created by the dramatic decrease of $S(\kappa)$, when $\kappa < \kappa_0$. The near coincidence of these cut-off limits creates the similar energy gaps between the ingoing neutron spectrum and the two cut-off limits, respectively. This similarity is to be expected because the structural change in going from the high temperature solid to the low temperature liquid is relatively small.

Acknowledgement

The author wants to thank Drs Göran Olsson and Ulf Dahlborg for performing some numerical computations on multiple scattering and Singwis model, respectively. The author also acknowledges Drs Sjögren, Sjödin and Ebbsjö for placing their data sets on aluminium at his disposal.

References

1. Unpublished data obtained 1958–59. Presented in Brookhaven, August 1959.
2. K. E. Larsson, U. Dahlborg, and D. Jovic, Collective atomic motions in liquid aluminium studied by cold neutron scattering, IAEA symposium in Bombay, 15–19 December, 1964, Proc. published as *Inelastic Scattering of Neutrons*, Vol. II, p. 117, Vienna (1965).
3. U. Dahlborg and K. E. Larsson, *Arkiv f. Fysik*, **33**, 271 (1966).
4. S. J. Cocking, A quasi-phonon treatment of coherent neutron scattering by liquid lead, IAEA symposium in Copenhagen, 20–25 May 1968, Proc. published as *Neutron Inelastic Scattering*, Vol. I, p. 463, Vienna (1968).
5. S. J. Cocking and Z. Guner, Comparative studies of slow neutron scattering by solid and liquid tin, IAEA symposium in Chalk River 10–14 September, 1962. Proc. published as *Inelastic Scattering of Neutrons in Solids and Liquids*, Vol. I, p. 237, Vienna (1963).
6. S. J. Cocking, Studies of liquid sodium by inelastic scattering of slow neutrons, IAEA symposium in Chalk River 10–14 September 1962. Proc. published as *Inelastic Scattering of Neutrons in Solids and Liquids*, Vol. I, p. 227, Vienna (1963).
7. G. H. Vineyard, *Phys. Rev.*, **110**, 999 (1958).
8. K. S. Singwi, *Phys. Rev.*, **136**, A969 (1964).
9. L. P. Kadanoff and P. C. Martin, *Ann. Phys. (N.Y.)*, **24**, 419 (1963).
10. R. Zwanzig and M. Bixon, *Phys. Rev.*, **A2**, 2005 (1970).

11. N. K. Ailawadi, A. Rahman, and R. Zwanzig, *Phys. Rev. A*, 1616 (1971).
12. R. C. Desai and S. Yip, *Phys. Rev.*, **166**, 129 (1968).
13. C. H. Chung and S. Yip, *Phys. Rev.*, **182**, 323 (1969).
14. S. W. Lovesey, *J. Phys. C: Solid St. Phys.*, **6**, 1856 (1973).
15. D. Pines in *Quantum Fluids*, edited by D. F. Brewer (North-Holland Publishing Company, Amsterdam, The Netherlands, 1966), p. 257.
16. K. N. Pathak and K. S. Singwi, *Phys. Rev.*, **A2**, 2427 (1970).
17. W. C. Kerr, *Phys. Rev.*, **174**, 316 (1968).
18. G. F. Mazenko, *Phys. Rev.*, **A3**, 2121 (1971); *Phys. Rev.*, **A5**, 2545 (1972); *Phys. Rev.*, **A7**, 209, 222 (1973), *Phys. Rev.*, **A9**, 360 (1974).
19. W. Götze and M. Lücke, *Phys. Rev.*, **A11**, 2173 (1975).
20. L. Sjögren and A. Sjölander, *Ann. Phys.*, **110**, 122, 156, 173, 421 (1978).
21. A. Rahman, *Phys. Rev.*, **136**, **A405** (1964); *Phys. Rev.*, **A9**, 1667 (1974).
22. D. Levesque and L. Verlet, *Phys. Rev.*, **A2**, 2514 (1970).
23. B. J. Alder and T. E. Wainwright, *Phys. Rev.*, **A1**, 18 (1970).
24. K. Sköld, J. M. Rowe, G. Ostrowski, and P. D. Randolph, *Phys. Rev.*, **A6**, 1107 (1972).
25. J. R. D. Copley and J. M. Rowe, *Phys. Rev.*, **A9**, 1656 (1974).
26. H. G. Bell, H. Möller-Wengtroffer, A. Kollmar, R. Stockmeyer, T. Springer, and H. Stiller, *Phys. Rev.*, **A11**, 316 (1975).
27. O. Söderström, J. R. D. Copley, B. Dorner, and J. B. Suck, unpublished data obtained in June 1978 at Grenoble.
28. J. R. D. Copley and S. W. Lovesey, The dynamic properties of monoatomic liquids, in Reports on *Prog. in Phys.*, **38**, pp. 482–515 (1975).
29. K. E. Larsson, U. Dahlborg, S. Holmryd, K. Otnes, and R. Stedman, *Arkiv f. Fysik*, **16**, 199 (1959).
30. L. Sjögren, *J. Phys. C: Solid St. Phys. Vol.*, **11**, 1493 (1978).
31. I. Ebbsjö, T. Kinell, and I. Waller, *J. Phys. C: Solid St. Phys. Vol.*, **11**, L501 (1978).
32. K. S. Singwi, K. Sköld, and M. P. Tosi, *Phys. Rev.*, **A1**, 454 (1970).
33. S. Sjödin, *J. Phys. C.* (1979) in press.
34. K. S. Singwi, *Physica*, **31**, 1257 (1965).
35. K. E. Larsson, U. Dahlborg, and S. Holmryd, *Arkiv f. Fysik*, **17**, 369 (1960).
36. B. N. Brockhouse, J. Bergsma, and B. A. Dasannacharya, Liquid dynamics from neutron spectrometry, IAEA symposium in Chalk River 10–14 September 1962. Proc. published as *Inelastic Scattering of Neutrons in Solids and Liquids*, Vol. I, p. 189, particularly p. 200, Vienna (1963).
37. B. N. Brockhouse, T. Arase, G. Caglioti, M. Sakamoto, R. N. Sinclair, and A. D. B. Woods, Crystal dynamics of lead, IAEA symposium in Vienna 11–14 October 1960. Proc. published as *Inelastic Scattering of Neutrons in Solids and Liquids*, p. 531, Vienna (1961).
38. T. Tsang and A. P. Maclin, *Phys. Rev.*, **A11**, 360 (1975).
39. T. Tsang and H. Tang, *Phys. Rev.*, **A15**, 1696 (1977).
40. D. J. Cocking, AERE Report, R5867, Thesis (1968).